Available online at www.sciencedirect.com

SCIENCE DIRECT®

Journal of Molecular Catalysis A: Chemical 202 (2003) 187–195

JOURNAL OF MOLECULAR CATALYSIS A: CHEMICAL

www.elsevier.com/locate/molcata

Structure and photocatalytic characteristics of TiO_2 film photocatalyst coated on stainless steel webnet

Jing Shang, Wei Li, Yongfa Zhu*

Department of Chemistry, Tsinghua University, Beijing 100084, PR China

Received 21 November 2002; accepted 27 February 2003

Abstract

High photocatalytic activities of TiO_2 films (50–360 nm) were coated on stainless steel webnet by the sol–gel method. Stainless steel webnet is a good substrate due to its large surface area, good ventilation for gases passing and good utilization of UV light. The TiO_2 films exhibited a uniform anatase structure with particle size about 10 nm. The photocatalytic activity of the TiO_2 film coated on stainless steel webnet can be related to its crystallization and thickness. With increasing of thickness of the TiO_2 film, the diffusion of the substrate was restricted from the surface and a more perfect crystallization of TiO_2 film was formed. Thicker and better crystallization of TiO_2 film resulted in its higher photocatalytic activity, which was evaluated by the photocatalytic oxidation of gaseous formaldehyde in a cylindrical flowing photoreactor. When the TiO_2 film thickness exceeds a certain value (about 250 nm), its photocatalytic activity remains unchanged. This indicated that only a certain thickness of the TiO_2 film was effective on the photocatalytic reaction.

Keywords: TiO_2 film; Stainless steel webnet; Photocatalytic activity; Formaldehyde; AES

1. Introduction

The photocatalyic activity of TiO_2 for the degradation of organic and inorganic air and water pollutants is a well-established phenomenon and constitutes a very interesting characteristic of this material [1–5]. Conventional powder photocatalysts, however, have a serious limitation—the need for post-treatment separation in a slurry system [6]. This can be overcome by immobilizing TiO_2 particles as thin films on a solid substrate. There are three techniques developed for coating of TiO_2 onto the surface of the support for fluidized- or packed-bed reactors, namely, impregnation, chemical vapor deposition (CVD) and sol–gel techniques [7]. Coating of TiO_2 by impregnation is widely used by most researchers because the technique is easy and does not require any complicated equipment, but the TiO_2 coating is not homogeneous and is easily detached from substrates. On the contrary, CVD and sol–gel techniques usually generate a relatively homogeneous TiO_2 coating. The sol–gel method of preparing TiO_2 films on substrates has many advantages over the CVD method [8], and, as a synthesis method to produce photocatalyst thin film from colloidal solutions, the method has almost exclusively been used until now.

The selection of a substrate may influence the activity, homogeneity and adhesion of the TiO_2 film photocatalyst. Therefore, various innovative substrates, such as stainless steel, glass, quartz, tile, paper,

* Corresponding author. Tel.: +86-10-627-83586; fax: +86-10-627-87601.
E-mail address: zhuyf@chem.tsinghua.edu.cn (Y. Zhu).

1381-1169/03/$ – see front matter © 2003 Elsevier Science B.V. All rights reserved.
doi:10.1016/S1381-1169(03)00200-0

non-woven fiber textiles, etc. have been developed [7–12]. The development of immobilized photocatalysts with high activity is still of great technological importance. However, film-type photocatalysts normally have lower surface areas than powdered ones, and the intrinsic photocatalytic activities of films are usually smaller than those of powders.

So far most of the research papers on TiO_2 films are only involved in the study of the structure of the crystal phase, the catalytic reaction, and so on. However, work is still necessary to elucidate the influence of all the parameters controlling the preparation of the supported catalysts and to determine how the characteristics of the resulting material can influence the photocatalytic process. Among these, the discussion of the interface reaction between the photocatalyst film and the substrate, the effect of the interface reaction on the structure and properties of the catalyst are far from complete. Since the interface reaction sometimes will have a serious influence on the properties of photocatalysts [13], it is quite necessary to make a further study.

In this work, a stainless steel webnet was employed as the substrate on which various thicknesses of TiO_2 films were coated using the sol–gel method. The webnet structure makes it possible to obtain a large surface area for TiO_2 films, as well as good ventilation for gases passing and good utilization of UV light. The structure of the TiO_2-coated stainless steel webnet was related to its photocatalytic activity, and tested in a flow photoreactor using formaldehyde as the model pollutant. The results confirm that the sol–gel method is a good way to prepare anatase TiO_2 film coated on stainless steel webnet firmly and this film exhibits high photocatalytic activity for the photocatalytic degradation of formaldehyde.

2. Experimental

2.1. Preparation of TiO_2 film photocatalyst

A 20 ml aliquot $Ti(OC_4H_9)_4$ (A.R.) was added dropwise at room temperature to 160 ml of ethanol (A.R.) and then 3 ml of $NH(OC_2H_5)_2$ was added to this solution. After stirring with an ultrasonic horn for 15 min, a light-yellow transparent solution was formed. After being gelatinized for 48 h, the precursor solution was mixed with 160 ml 98% (v/v) ethanol solution. Sealed and gelatinized for 72 h, a sol with a certain viscosity was obtained.

The stainless steel webnet was selected as a support for catalyst because of its flexibility to be engineered and its resistance to various corrosions. Additionally, the large surface area of the stainless steel webnet can provide more active sites for the deposition of TiO_2 than general supports. The stainless steel webnet was obtained from Haidian Hardware Store of Beijing in China. In the experiment, 60 mesh stainless steel webnet was first rinsed by 0.1 M hydrochloric acid and distilled water. Then, a piece of pre-dried stainless steel webnet, 16 cm × 10.5 cm, was dipped into the sol for 10 s and then rotated at a high speed to form a wet gel film. After drying at 80 °C, the substrate coated with a TiO_2 dry-gel film was heated to 400 °C at 5 °C min^{-1}, and calcined at 400 °C for 10 min in an air flow oven. The thickness of the TiO_2 film was adjusted by repeating the cycle from dipping to heat treatment. The thicknesses of the TiO_2 films subjected to 1–4 cycles were 50, 140, 250 and 360 nm (determined by AES analyses), respectively.

2.2. Characterization of TiO_2 film photocatalysts

The morphologies of the TiO_2 films were taken by using a KYKY2000 scanning electron microscope (SEM). A Hitachi H-800 transmission electron microscope (TEM) was used to measure the particle size. A small part of the TiO_2 film was sonicated in a 50% ethanol solution (v/v) for 20 min. The resulting solution was dipped onto a piece of Cu net followed by a TEM analysis. Raman spectra of the TiO_2 films with different coating cycles were conducted on a Renishaw RM1000 spectrometer, and the wavelength of the laser light was 514 nm. The Auger electron spectroscopy (AES) technique was used to determine the thickness of the TiO_2 films subjected to different cycles. Also, the interface diffusion and reaction could be observed. AES spectra were obtained using a PHI 610 scanning auger microscopy system. The beam voltage was 3.0 kV and the beam current was 0.5 μA. The electron beam was incident at an angle of 60° with respect to the specimen surface in order to make the sample surface perpendicular to the ion beam. During the depth profile analysis, the energy and beam current of the Ar ion beam were 3.0 keV and 6 μA, respectively. The

beam diameter was 1 mm and the sputtering rate was approximately 30.0 nm min^{-1} for a thermally oxidized SiO_2 thin film.

2.3. Photocatalytic reaction

The schematic diagram of the photoreactor system used in this study is shown in Fig. 1(A). It consisted of an air carrier gas contaminated with formaldehyde. The concentration of formaldehyde in the contaminated atmosphere was obtained by vaporization of formaldehyde liquid using pre-determined values of flow rate controlled by mass flow controllers. The mixture was then forced to flow through the photoreactor (with TiO_2-coated webnet) where it was destroyed. Fig. 1(B) is a schematic drawing of the employed cylindrical UV photoreactor. The distance in the radial direction within the cylindrical UV reactor is represented by r. L is the length of the photoreactor. The reflection or refraction of light at all interfaces is assumed to be negligible. The photoreactor was constructed from stainless steel with an effective volume of about 0.6 l. TiO_2-coated webnet was wound and fixed to the inner concentric hollow frame. An 8 W 254 nm bactericidal lamp was used as light source and the radiation power was measured to be 1500 μW cm^{-2} 2.5 cm away from the lamp. The distance between the lamp and the TiO_2-coated webnet was about 2.5 cm and the total effective irradiation area of the TiO_2-coated webnet was about 120 cm^2. A control sample was run by flowing the contaminated air through a catalyst-free reactor, in order to eliminate the possibility of homogeneous photodestruction (direct photolysis) of formaldehyde. In the experiment, the gas flow rate was 156 ml min^{-1}.

Reactor influent and effluent samples were collected using an sampling valve (SV) and analyzed in an SP-502 gas chromatograph (GC) equipped with a 2 m stainless steel column (GDX-403) and a flame ionization detector (FID). In a typical test, an air stream contaminated with the formaldehyde under study was passed through the photoreactor in the absence of UV illumination until the gas–solid adsorption equilibrium was established. After the adsorption process reached equilibrium, as indicated by identical inlet–outlet formaldehyde concentration, the UV lamp was turned on and the outlet gas was sampled.

3. Results and discussion

3.1. Texture of TiO_2 films

The surface morphologies of the stainless steel webnet coated with and without TiO_2 are shown in Fig. 2. It can be seen that TiO_2 films of 50–250 nm thicknesses can be uniformly coated on stainless steel webnet. However, when the film thickness increased to 360 nm, some aggregates began to form (as shown in Fig. 2(D)).

Fig. 3 shows TEM images of the TiO_2 films. The TiO_2 films are made up of spherical particles and the particle size is about 10 nm. Based on Fig. 3(A) and (B), the particle size did not change much with increasing film thickness. This indicates that the thickness of the TiO_2 film does not affect the particle size, at least up to a thickness of 360 nm.

3.2. Crystallization of TiO_2 films

Raman spectroscopy was used to investigate the crystallization of the TiO_2 film on the stainless steel webnet. Fig. 4 shows Raman spectra for different thickness TiO_2 films coated on webnet as well as that of the substrate. It was reported that peaks at 142, 404, 516 and 635 cm^{-1} are characteristic of anatase TiO_2 [14–16]. So the TiO_2 films here coated on the stainless steel webnet are anatase. It is commonly observed that the optical edge shifts to the blue, which is often attributed to the quantum size effect [17]. This effect is much more pronounced for the peak at 142 cm^{-1}, the main peak of anatase titania. The Raman shift increases from 142 to 145 cm^{-1}, indicating the diameter of the TiO_2 is about 10 nm according to the expressions provided by Kelly et al. [14], Doss and Zallen [18]. This result is consistent with the TEM observations.

Based on Fig. 4, TiO_2 films with a thickness from 50 to 140 nm exhibit weak anatase peaks, and iron oxide with its peak at 671 cm^{-1} is detected for these two samples. With increasing thickness, the anatase peaks become more intense and the iron oxide peak disappears. This indicates that a better crystallization of the anatase TiO_2 is resulted from a thicker TiO_2 film, which covers the diffusion of iron oxide. This can be further verified by AES analyses.

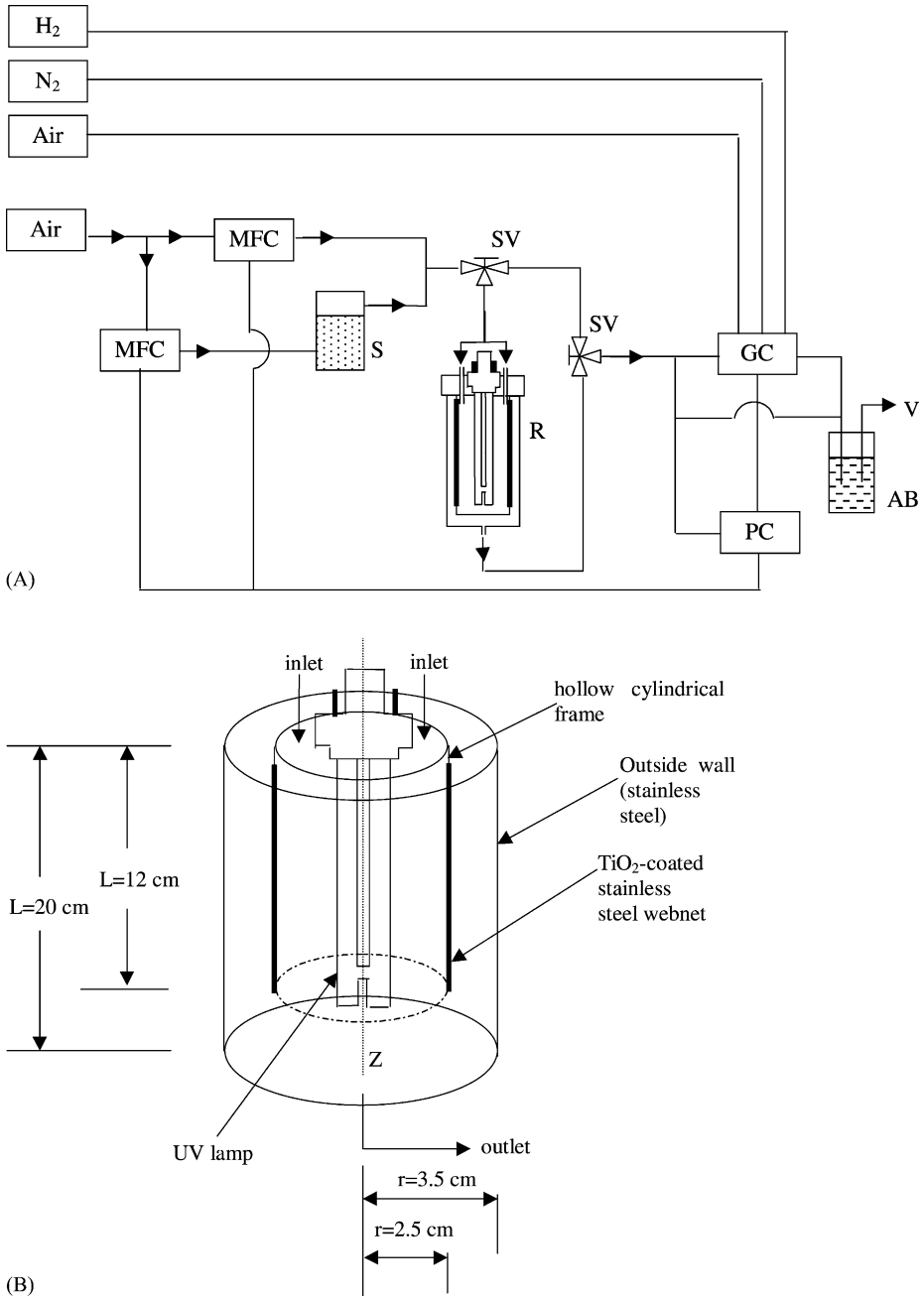

Fig. 1. (A) Schematic of the experimental apparatus. MFC: mass flow controller; S: saturator with formaldehyde; SV: sampling valve; R: reactor; GC: gas chromatography; PC: personal computer; AB: absorption bottle; V: vent; (B) photocatalytic reactor geometry.

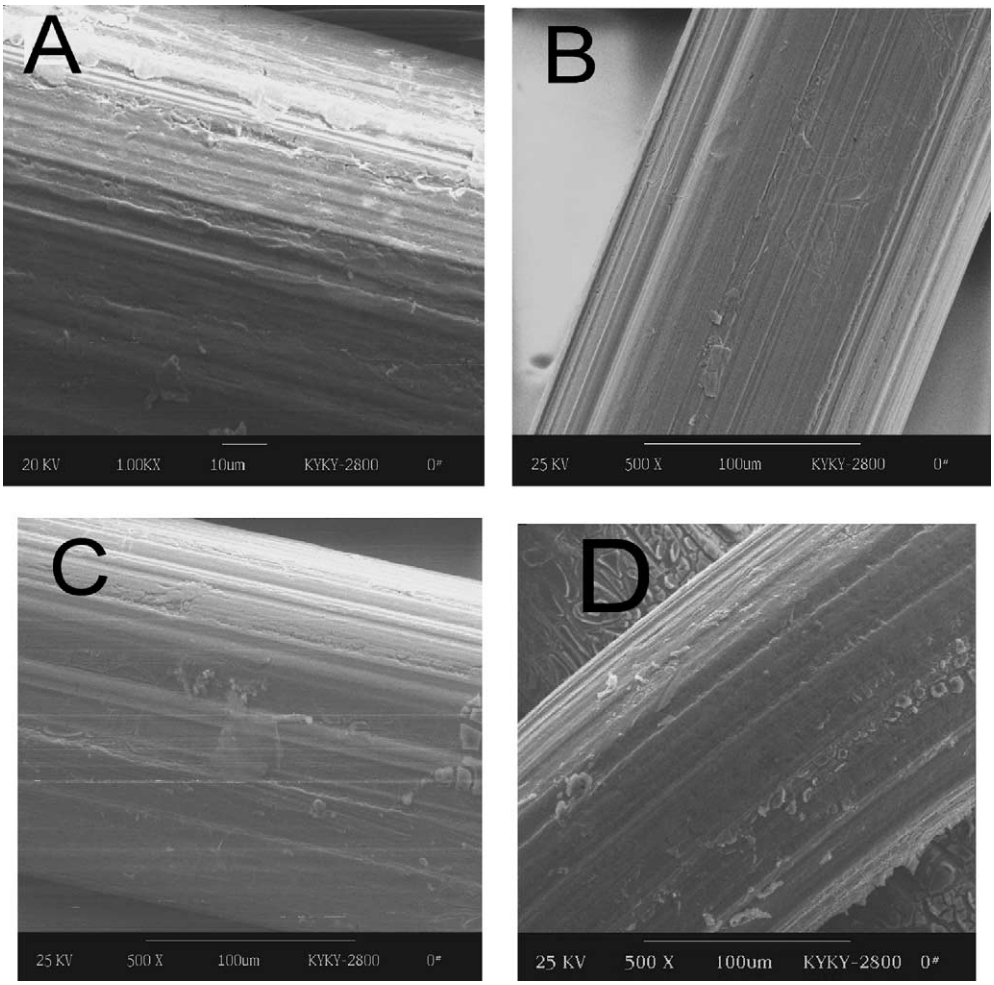

Fig. 2. SEM images of (A) stainless steel webnet substrate; (B) 50 nm thickness TiO_2 film; (C) 250 nm thickness TiO_2 film and (D) 360 nm thickness TiO_2 film.

3.3. *Thickness and interface diffusion of TiO_2 films*

Fig. 5 corresponds to AES depth profile spectra of the TiO_2 film/stainless steel webnet samples. As has been outlined in the experimental section, the thickness of the TiO_2 films treated for 1–4 cycles can be calculated from Fig. 5, with values of 50, 140, 250 and 360 nm, respectively.

As shown in Fig. 5, the interlayers between the TiO_2 films and the substrates was observed and a certain amount of Fe was found in the TiO_2 layers. When the film thickness was 50 nm, Fe diffused to the surface of the TiO_2 film, with a concentration of 4% on the surface. Fe did not diffuse to the surface of the TiO_2 film when the film thickness was over 50 nm. It was found by Zhu et al. [13] that Fe in a stainless steel substrate diffused into a TiO_2 film and reacted with O_2 that diffused from the air, forming an interlayer of iron oxide during an annealing treatment. However, the diffusion of iron oxide did not change the electronic structure of the TiO_2 [13]. The existence of iron oxide also has been proven by Raman spectroscopy (shown in Fig. 4). Based on Fig. 5, the distribution of the Ti concentration with depth in the TiO_2 layer is homogeneous; however, Ti also diffuses into the stainless steel webnet substrate but the concentration

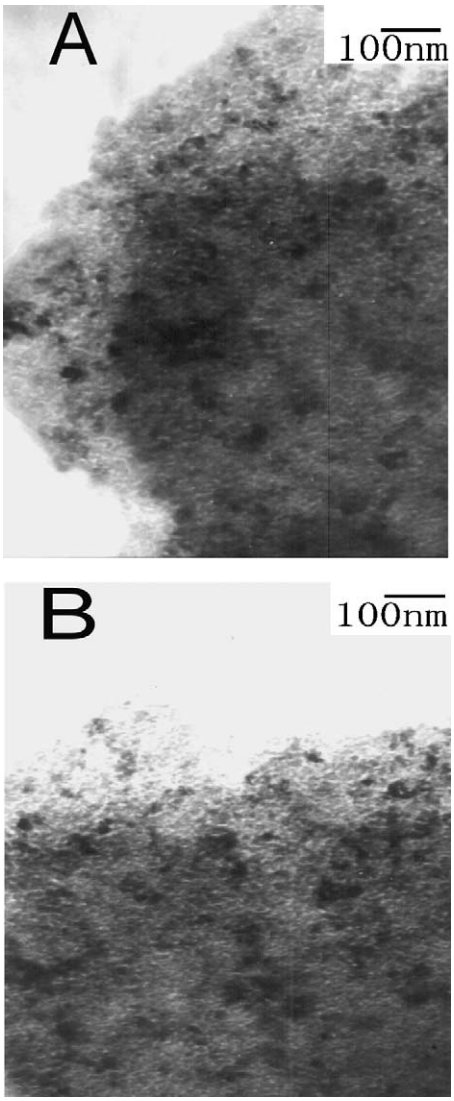

Fig. 3. TEM images of (A) 50 nm thickness TiO_2 film and (B) 360 nm thickness TiO_2 film.

is very low. The above results suggest that diffusion between the TiO_2 layer and the stainless steel webnet has taken place, making the coating of the TiO_2 layer on the stainless steel webnet firm.

Combining the results of AES and Raman spectra, it can be confirmed that the incorporation of Fe accounts for the poor crystallization of TiO_2 when the film thickness is less than 140 nm. However, the diffusion of substrate Fe can be banned from the surface

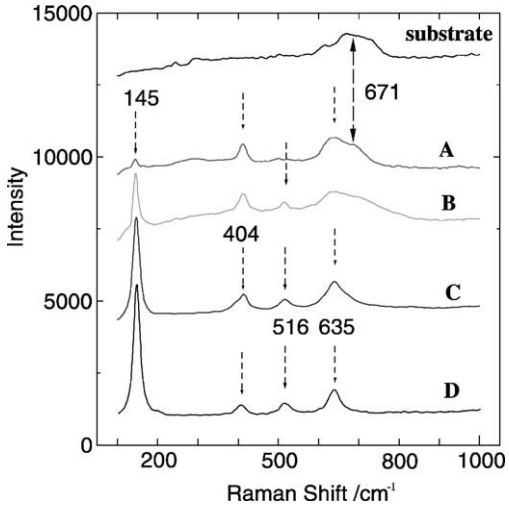

Fig. 4. Raman spectra of (A) 50 nm thickness TiO_2 film; (B) 140 nm thickness TiO_2 film (C) 250 nm thickness TiO_2 film and (D) 360 nm thickness TiO_2 film. Substrate is the stainless steel webnet after calcining at 400 °C for 10 min in an air flow oven.

by increasing the thickness of the TiO_2 layer. This results in more perfect crystallization of the TiO_2 films, as shown by the Raman spectra. That is to say, the influence of Fe diffusion on the crystallization of the TiO_2 film is negligible with the increase of TiO_2 film thickness. In addition, the film is stably attached to the stainless steel webnet owing to the diffusion.

3.4. Photocatalytic activity of TiO_2 films

In Fig. 6, the variation of the degraded concentrations of formaldehyde with irradiation time for different thicknesses of the TiO_2 films are given. Blank experiments indicated that photocatalytic reaction did not proceed in the absence of either TiO_2 or UV light. However, once there were both TiO_2 and UV irradiation, formaldehyde could be photocatalytically degraded. After the gas–solid adsorption process reached equilibrium, with the initial concentration of formaldehyde being 6.25×10^{-5} mol l^{-1}, the UV lamp was turned on. As can be seen from Fig. 6, the degraded concentration of formaldehyde increased with both the irradiation time and film thickness. The increase was more pronounced at the beginning of the irradiation (as well as with increasing film thickness) and then leveled off. A new steady state was achieved about

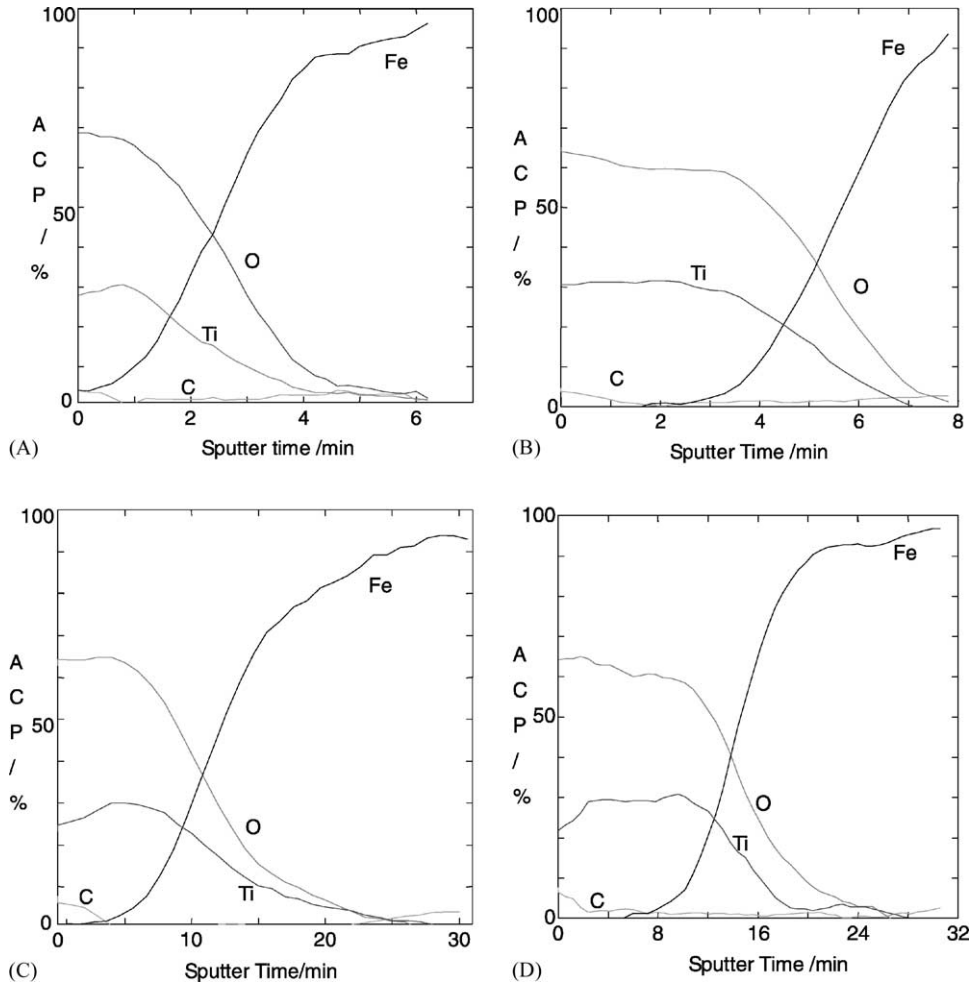

Fig. 5. The AES depth profile spectra of the TiO_2 films/stainless steel webnet samples treated for (A) 1 cycle (50 nm); (B) 2 cycles (140 nm); (C) 3 cycles (250 nm) and (D) 4 cycles (360 nm).

5 h after the lamp was turned on. Also an increase in the degraded concentration of formaldehyde was not obvious after the film thickness reached 250 nm.

As discussed above, it can be concluded that film thickness of TiO_2-coated webnet has an influence on its crystallization, diffusion, and further on its photocatalytic activity. The structure characteristics of the TiO_2-coated webnet can be related to its photocatalytic activity. Based on the experimental data, one could clearly find such a regularity: when film thickness ranged from 50 to 250 nm, the activity of the photocatalyst increased with increasing film thickness; when the film was thicker than 250 nm, the activity of the photocatalyst changed little and was almost independent of the film thickness. The relationship of the photocatalytic activity to film thickness can be explained well by analyzing both the crystallization and light absorption of the TiO_2 film photocatalyst. The TiO_2 film photocatalyst with 50 nm thickness exhibits the lowest activity, which can be explained by the following two factors: (1) poor crystallization of the anatase TiO_2 due to the diffusion of Fe to the film surface. The diffusion of Fe into the TiO_2 layer was unavoidable during the baking of the photocatalyst in an oven at 400 °C. Especially when the thickness of the TiO_2 film was 50 nm, Fe diffused to the surface of

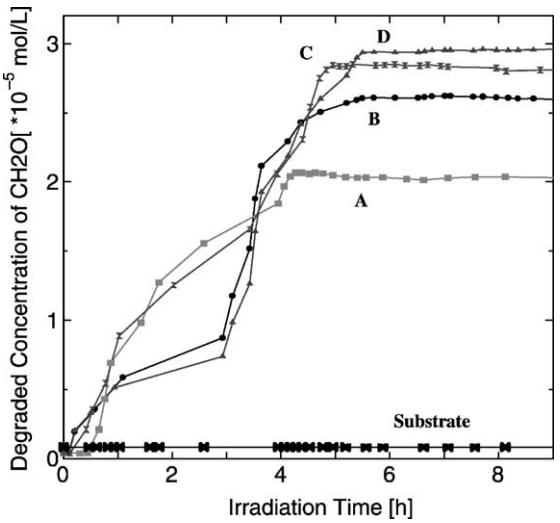

Fig. 6. The variations of the degraded concentration of formaldehyde with irradiation time for different thicknesses of TiO_2 films. (A) 50 nm thickness TiO_2 film; (B) 140 nm thickness TiO_2 film (C) 250 nm thickness TiO_2 film and (D) 360 nm thickness TiO_2 film. Substrate is the stainless steel webnet after calcining at 400 °C for 10 min in an air flow oven.

TiO_2 film. As a direct consequence of the Fe diffusing into the TiO_2 layer, the growth of crystalline TiO_2 grains is inhibited, which reduces the intrinsic activity of the photocatalyst; (2) there is weak light absorption due to the thin TiO_2 film. As we know, under the condition that both UV light with suitable energy and oxygen are available, reactive oxygen species such as O_2^-, O^-, O, $^\bullet OH$ and $HO_2^\bullet$ are generated on the surface of TiO_2 [19,20]. Both holes and reactive oxygen species such as $^\bullet OH$ have been proposed as the species responsible for initiating the oxidative attack on organic compounds. Normally, the more absorbed light, the more reactive oxygen species are generated on the surface of the photocatalyst, and consequently the more active the photocatalyst is. Fifty nanometer thickness TiO_2 film photocatalysts cannot absorb enough light for the formation of enough reactive oxygen species to take part in the photocatalytic reaction, resulting in poor photocatalytic activity.

When the film thickness was increased from 50 to 250 nm, the photocatalytic activity could be enhanced. On the one hand, the diffusion of Fe to the surface of the TiO_2 film could be decreased by increasing the thickness of TiO_2 layer. As a consequence, the crystalline grains in the TiO_2 layer exposed to the light became more perfect. On the other hand, the number of reactive oxygen species increased, due to the increase in thickness of the TiO_2 film and resulted in an increase in the light-harvesting capacity.

For the two TiO_2 films with thickness being 250 and 360 nm, Fe is restricted from diffusing to the surface and consequently there are not too much difference in the crystallization of the two photocatalysts. It was interesting to note that the photocatalytic activity of the two samples changed little although the thickness increased continually. That is to say, a certain thickness of the TiO_2 film was needed to guarantee its perfect crystallization and correspondingly its photocatalytic activity, and after that only a limited thickness of the TiO_2 layer (close to 250 nm in this case) was effective for the photocatalytic oxidation reaction. As we know, carriers (e^- and h^+) photogenerated in the TiO_2 can transfer to the surface of TiO_2 where trapping reactions occur with above reactive oxygen species. However, if the carriers formed in the photocatalyst cannot be transported to the surface of the photocatalyst in time, they will not contribute to the photocatalytic reaction. Most of the carriers recombine with each other within a few nanoseconds [1]. According to Tachibana et al. [21], an appropriate light-scattering magnitude in the TiO_2 film originating from the particle sizes and their distribution, and the film thickness are key parameters in controlling the electron-transfer yield as well as the light-harvesting efficiency. Based on our experimental data, it was indicated that the light-harvesting efficiency reached saturation with a certain thickness of the TiO_2 film. Therefore, the photocatalytic activity of a TiO_2 film thicker than 250 nm remains constant.

Table 1 shows the effect of the initial concentration of formaldehyde on photocatalytic activity using the 250 nm thick TiO_2 film as a photocatalyst. It was found that with increasing the concentration of formaldehyde in the inlet gas flow, the degraded concentration of formaldehyde increased to a certain extent before reaching a constant value. This probably resulted from the limited and fixed number of reactive sites on the surface of TiO_2 available for the adsorption of formaldehyde. Similar results were observed and discussed for the decomposition of toluene over TiO_2 with saturated adsorption under fixed active sites [22], as well as for the photocatalytic degradation of

Table 1
Effect of initial concentration of formaldehyde on photocatalytic activity using a 250 nm thickness TiO_2 film as a photocatalyst

Initial concentration of formaldehyde ($\times 10^{-5}$ mol l^{-1})	Degraded concentration of formaldehyde ($\times 10^{-5}$ mol l^{-1})
1.25	1.25
2.08	2.08
2.50	2.50
4.17	2.79
5.00	2.79
6.25	2.79

TCE [7]. When the concentration of formaldehyde was below its saturated value, formaldehyde could be completely degraded to CO_2 and H_2O. As can be seen from Table 1, the maximum degraded concentration of formaldehyde on a uniform anatase TiO_2 film was 2.79×10^{-5} mol l^{-1}, the flow rate of 156 ml min^{-1} being constant during the experiment.

It was found that the photocatalytic activity of TiO_2-coated stainless steel webnet was maintained at a constant value for long periods of reaction time, usually more than 200 h, and could be assumed to be constant during the course of reaction. This indicates that the deposited TiO_2 is not deactivated during the reaction and can be re-utilized in subsequent runs. This is an important feature for its potential use as an immobilized catalyst working in batch or flow photoreactors.

4. Conclusion

A good controlled morphology and crystalline phase of TiO_2 film (50–360 nm) with a high photocatalytic activity can be obtained by sol–gel method coated on stainless steel webnet.

Thicker and better crystallization of TiO_2 film results in its higher photocatalytic activity. However, the thickness of the TiO_2 film has a saturation value for the photocatalytic reaction due to the saturation of light-harvesting efficiency.

This paper shows that the adhesion of TiO_2 on a stainless steel webnet is of good quality and can be reused in subsequent runs.

Acknowledgements

This work was partly supported by the Chinese National Science Foundation (20071021), the Excellent Young Teacher Program of MOE. P.R.C. and the Visiting Scholar Foundation of Key Lab in Beijing Universtiy.

References

[1] M.R. Hoffmann, S.T. Martin, W. Choi, D.W. Bahnemann, Chem. Rev. 95 (1995) 69.
[2] A. Fujishima, T.N. Rao, D.A. Tryk, J. Photochem. Photobiol. C: Photochem. Rev. 1 (2000) 1.
[3] A.L. Linsebigler, G. Lu, J.T. Yates Jr., Chem. Rev. 95 (1995) 735.
[4] J. Peral, X. Domentech, D.F. Ollis, J. Chem. Technol. Biotechnol. 70 (1997) 117.
[5] D.F. Oills, E. Pelizzetti, N. Serpone, Environ. Sci. Technol. 25 (1991) 1522.
[6] K. Tennakone, I.R.M. Kottegoda, J. Photochem. Photobiol. A: Chem. 93 (1996) 79.
[7] Y. Ku, C.M. Ma, Y.S. Shen, Appl. Catal. B: Environ. 34 (2001) 181.
[8] J.C. Yu, J. G Yu, J.C. Zhao, Appl. Catal. B: Environ. 36 (2002) 31.
[9] Y.F. Zhu, L. Zhang, W.Q. Yao, L.L. Cao, Appl. Surf. Sci. 158 (2000) 32.
[10] A. Ferandez, G. Lassaletta, V.M. Jimenze, A. Justo, A.R. Gonzalze, J.M. Hermann, H. Tahiri, Y. Ait-Ichou, Appl. Catal. B: Environ. 7 (1995) 49.
[11] J.R. Bellobona, A. Carrana, B. Bami, A. Gazzotti, J. Photochem. Photobiol. A. 84 (1994) 83.
[12] J. Sobate, M.A. Anderson, H. Kikkawa, Q. Xu, S. Cervera-March, C.G. Hill Jr., J. Catal. 134 (1992) 36.
[13] Y.F. Zhu, L. Zhang, L. Wang, Y. Fu, L.L. Cao, J. Mater. Chem. 11 (2001) 1864.
[14] S. Kelly, F.H. Pollak, M. Tomkiewicz, J. Phys. Chem. B. 101 (1997) 2730.
[15] U. Balachandran, N.G. Eror, J. Solid. State. Chem. 42 (1982) 276.
[16] G. Busca, G. Ramis, J. Chem. Soc., Faraday Trans. 90 (1994) 3181.
[17] Z.L. Xu, J. Shang, Ch.M. Liu, Ch.L. Kang, H.Ch. Guo, Y.G. Du, Mater. Sci. Eng. B. 56 (1999) 211.
[18] C.J. Doss, R. Zallen, Phys. Rev. B. 48 (1993) 15626.
[19] T. Ibusuki, K. Takeuchi, J. Mol. Catal. 88 (1993) 93.
[20] D.E. Park, J.L. Zhang, K. Ikeue, H. Yamashita, M. Anpo, J. Catal. 185 (1999) 114.
[21] Y. Tachibana, K. Hara, K. Sayama, H. Arakawa, Chem. Mater. 14 (2002) 2527.
[22] T.N. Obee, S.O. Hay, Environ. Sci. Technol. 31 (1997) 2034.